Molecular Crystals and Liquid Crystals

Publication details, including instructions for authors and subscription information:
http://www.tandfonline.com/loi/gmcl20

Structure and Electronic Property of C_{60} and Rb_xC_{60} Thin Films Analyzed by STM/STS Technique

Yusei Maruyama [a], Kyoujiro Ikeda [b], Tomohiro Yoshikawa [b], Junko Inoue [b], Takashi Maeyama [b] & Mikio Watanabe [b]

[a] Research Center for Micro-Nano Technology, Hosei University, Midorichou, Koganei, Tokyo, Japan

[b] Department of Materials Chemistry, College of Engineering Hosei University, Kajinochou, Koganei, Tokyo, Japan

Version of record first published: 22 Sep 2010

To cite this article: Yusei Maruyama, Kyoujiro Ikeda, Tomohiro Yoshikawa, Junko Inoue, Takashi Maeyama & Mikio Watanabe (2007): Structure and Electronic Property of C_{60} and Rb_xC_{60} Thin Films Analyzed by STM/STS Technique, Molecular Crystals and Liquid Crystals, 466:1, 113-127

To link to this article: http://dx.doi.org/10.1080/15421400601150254

Mol. Cryst. Liq. Cryst., Vol. 466, pp. 113–127, 2007

ISSN: 1542-1406 print/1563-5287 online
DOI: 10.1080/15421400601150254

Structure and Electronic Property of C_{60} and Rb_xC_{60} Thin Films Analyzed by STM/STS Technique

Yusei Maruyama
Research Center for Micro-Nano Technology, Hosei University, Midorichou, Koganei, Tokyo, Japan

Kyoujiro Ikeda
Tomohiro Yoshikawa
Junko Inoue
Takashi Maeyama
Mikio Watanabe
Department of Materials Chemistry, College of Engineering, Hosei University, Kajinochou, Koganei, Tokyo, Japan

Scanning tunneling microscopy (STM) studies for C_{60} crystalline thin films at low temperatures have revealed the orientation ordering of C_{60} molecules in the C_{60} crystal at low temperatures. In the rubidium-doped C_{60} films, the results of a spatially resolved scanning tunneling spectroscopy (STS) study have clearly indicated the possible hybridization of the wave functions of rubidium ions with those of C_{60} molecules, which causes the metallic nature of the compound.

Keywords: electron density of states; fullerenes; fullerides; orientation ordering; scanning tunneling microscopy; scanning tunneling spectroscopy

INTRODUCTION

It is well known that a C_{60} molecule has highly symmetric spherical structure [1] and is freely rotating with very high speed in a crystal at room temperature [2]. The rotational motion of C_{60} molecules in a crystal causes various phases of intermolecular orientation ordering depending on the temperatures. A first-order structural phase transition of the rotational freedoms from free to ratchet rotation occurs

Address correspondence to Yusei Maruyama, Research Center for Micro-Nano Technology, Hosei University, Midorichou, Koganei, Tokyo 184-0003, Japan. E-mail: maruyama@k.hosei.ac.jp

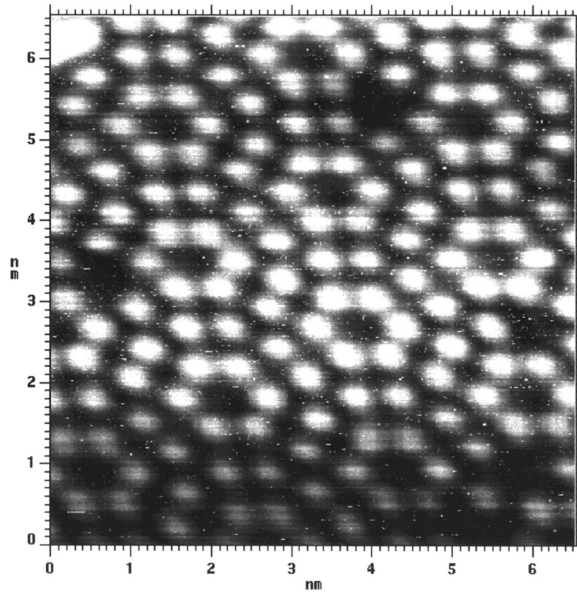

FIGURE 1 Typical STM image of the reconstructed [7 × 7] structure on the Si (111) surface of the single-crystal substrate used in this study.

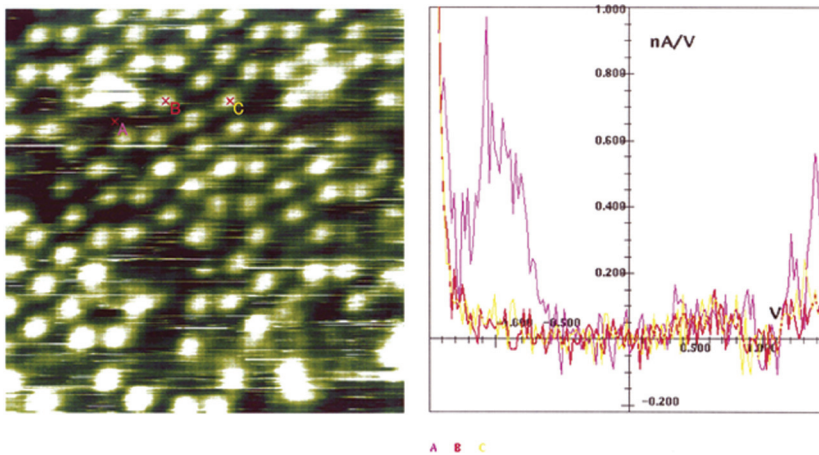

FIGURE 2 Site-selected STS measurement on the [7 × 7] structure of Si (111) surface. The x_A, x_B and x_C sites on the left indicate the selected sites for the tunneling spectra in this STS operation, which are shown on the right where A (pink), B (red), and C (yellow) spectra correspond to x_A, x_B and x_C sites, respectively.

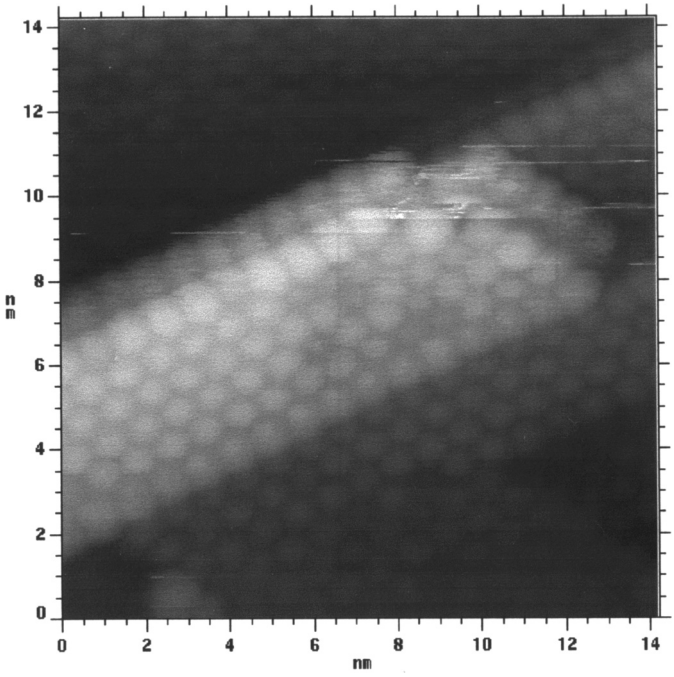

FIGURE 3 Typical STM image of the C_{60} thin films deposited on the Si (111) surface in the average thickness of one or two molecular layers thick.

at 260 K [3], and below ca. 90 K the rotational motion is almost frozen, leaving a kind of static disorder [4]. STM studies on the orientation ordering of C_{60} were carried out for ultrathin C_{60} layers on silicon or metal single-crystal substrates [5,6]. In these cases, the dangling bonds of silicon surface or the charge transfer from metal surface may be effective for hindering the rotation of C_{60} molecules. In our case a few or more molecular layer C_{60} films were deposited on a silicon single-crystal substrate and observed by an STM at low temperatures comparing with the images at room temperature. Clear indication of freezing of molecular rotation and a fairly definite orientation ordering were obtained at low temperatures. The correlation of the STM images with the calculated molecular orbital patterns is discussed.

Another subject of this report is an STM/STS study on the metallic nature of alkali metal C_{60} complex solids. Alkali metal-doped C_{60} solids have been known to be metallic conductors [7] and superconductors at low temperatures [8] when they are properly doped [9]. The main role of alkali metal is believed to be the electron donation to C_{60} molecules because of its relatively low ionization potential energy.

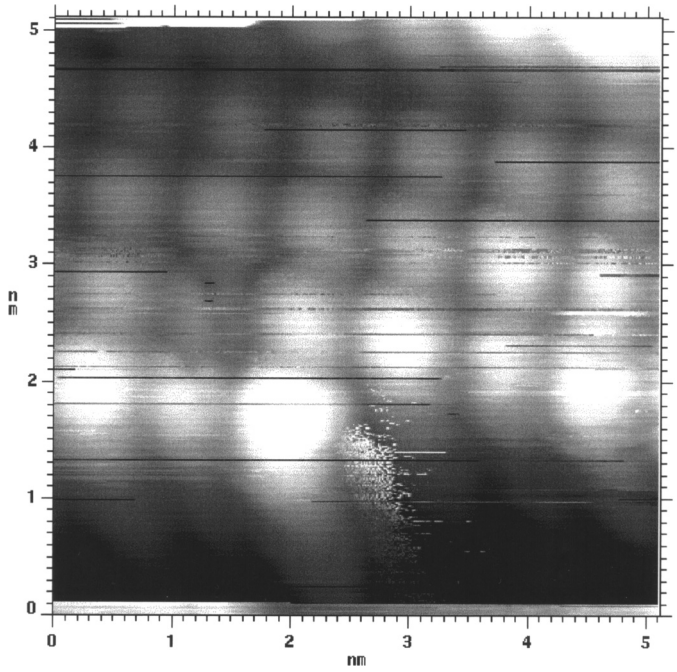

FIGURE 4 STM image of the C_{60} thin film of several molecular layers thick ($\sim$7 nm) observed at room temperature.

In this work, we have aimed to clarify the more detailed functions of the alkali metal to transform the electronic character of the solid from insulator to metal by the doping reaction. We have directly observed the change of the electron density of states due to doping by applying an STS technique in the space- and energy-resolved way.

EXPERIMENTAL

In both experiments, an ultrahigh vacuum variable-temperature STM system combined with a molecular-beam-epitaxial deposition (MBED) chamber (Omicron Inc.) was used. The base pressures in the STM and MBED chamber were $\sim 10^{-12}$ Torr and $\sim 10^{-11}$ Torr, respectively. The temperature of a sample at the STM stage can be lowered down to $\sim$20 K using a liquid helium flowing system. In the first place, the (111) surface of silicon single crystal was cleaned and reconstructed to the $[7 \times 7]$ structure by a proper heat treatment, which was confirmed by STM observation (Fig. 1) and STS measurement (Fig. 2).

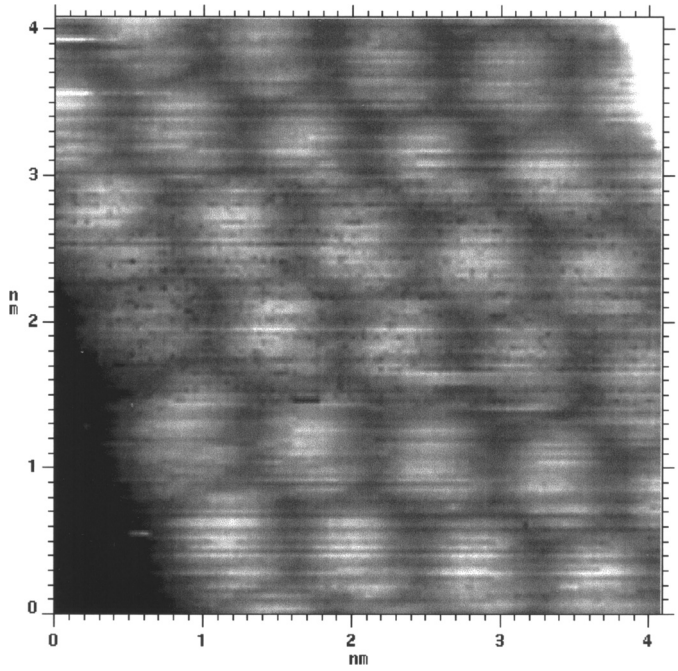

FIGURE 5 STM image of the surface of the film in Fig. 4 at a little higher magnification.

On this type of silicon surfaces, C_{60} ultra-thin films were deposited by the thickness of a monomolecular layer (Fig. 3) or several molecular layers (Fig. 4). The average thickness of the film was monitored by a quartz oscillator. Thus even in the monomolecular layer film, the microstructure is not homogeneous and seems to be rather island-like (Fig. 3), and the thicker film seems to have well-developed crystalline domains (Fig. 4).

RESULTS AND DISCUSSION

Each C_{60} molecule on the crystalline surface shown in Fig. 4 is believed to be so freely rotating at room temperature that even in higher magnified images the molecules seem to be spherical balls without any internal structure (Fig. 5). However, at low temperatures, $\sim$25 K, the images of each molecule at the same magnification showed clearly different views (Fig. 6) from those in Fig. 5. The STM images strongly depend on the spatially local distribution of the electron density of states of the surface at the fixed energy, which is set by the bias

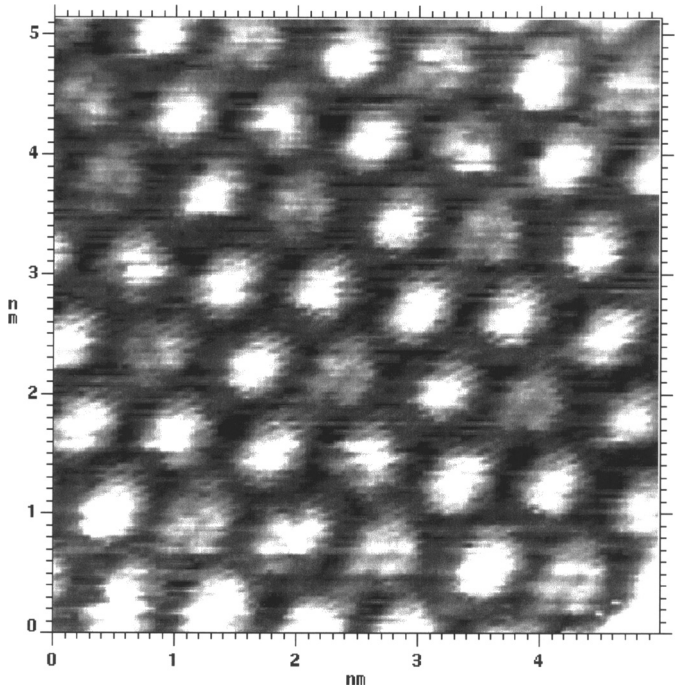

FIGURE 6 STM image of the same surface of the C_{60} thin film as in Fig. 4 observed at 25 K.

voltage between the probe tip and the sample surface. Thus, the STM images of Fig. 6 may represent the absolute values of the amplitudes at the each carbon atom site of the molecular orbital at the fixed energy corresponding to the bias voltage, which were viewed from a fixed direction if the molecule was forced to be set in a fixed orientation without any free rotation at low temperatures. Furthermore, the STM image patterns of the same molecule were clearly changed depending on the bias voltages as shown in Figs. 7a and b. At the voltage of 3.5 V (eV), the pattern showed star-like trigonal symmetry (Fig. 7a), but at the voltage of 2.5 V (eV), it changed to dual-stripe pattern (Fig. 7b). In this case, we observed the different molecular orbital of the molecule in same orientation corresponding to the higher and lower bias voltages. The higher voltage pattern may originate from the molecular orbital of h_g symmetry at around 4 eV in Fig. 8, which is a typical Huckel molecular orbital diagram for the π-electrons of a C_{60} molecule. Accordingly, the lower voltage pattern may come from the t_{1g} at around 3 eV. A simple molecular orbital calculation for the

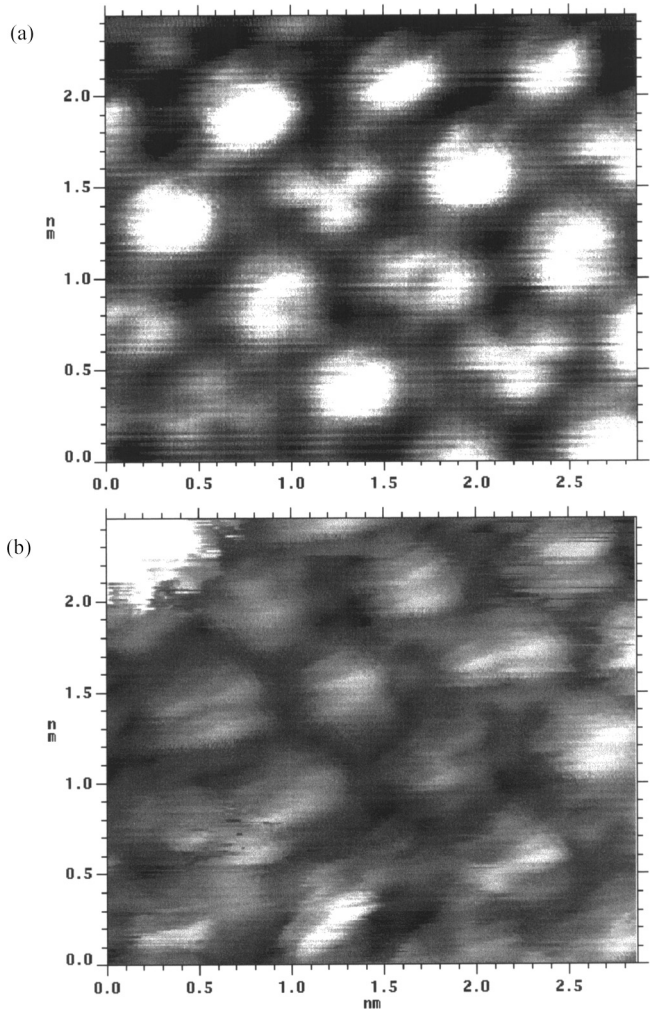

FIGURE 7 STM images of the surface of the C_{60} thin film at 25 K observed at different bias voltages: (a) 3.5 V and (b) 2.5 V.

distribution of the wave functions at each atomic site provided the visual image patterns corresponding to the each voltage. The trigonal pattern is consistent with the molecular orientation shown in Fig. 9a. The spherical pattern may come from the different molecular orientation of the same orbital, h_g, as shown in Fig. 9b. The dual-stripe pattern at the lower voltage may correspond to the model of the same molecular orientation at the different orbital, t_{1g}, as shown in Fig. 9c.

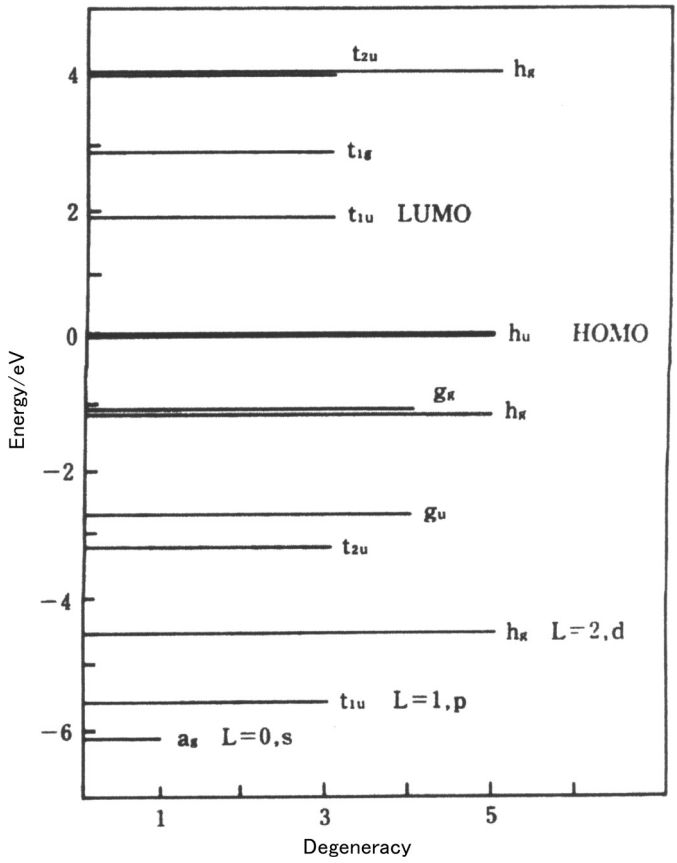

FIGURE 8 Energy-levels diagram of the molecular orbital of π electrons in the C_{60} molecule.

FIGURE 9 (a) Calculated molecular orbital pattern (the h_g level around 4 eV in Fig. 8) at the fixed orientation, which may correspond to the observed trigonal symmetry image in Fig. 7a. The arrow lines are the guide for eye to show the trigonal symmetry. (b) The molecular orbital pattern of the same level as in Fig. 9a viewed in some different orientation from that in Fig. 9a, which shows a diffuse spherical pattern. (c) The calculated molecular orbital pattern corresponding to the same molecular orientation as that in Fig. 9a but at different energy level (t_{1g} around 3 eV in Fig. 8), which may correspond to the observed dually split image in Fig. 7b. The lines are the guide for the eye to show the dually split image.

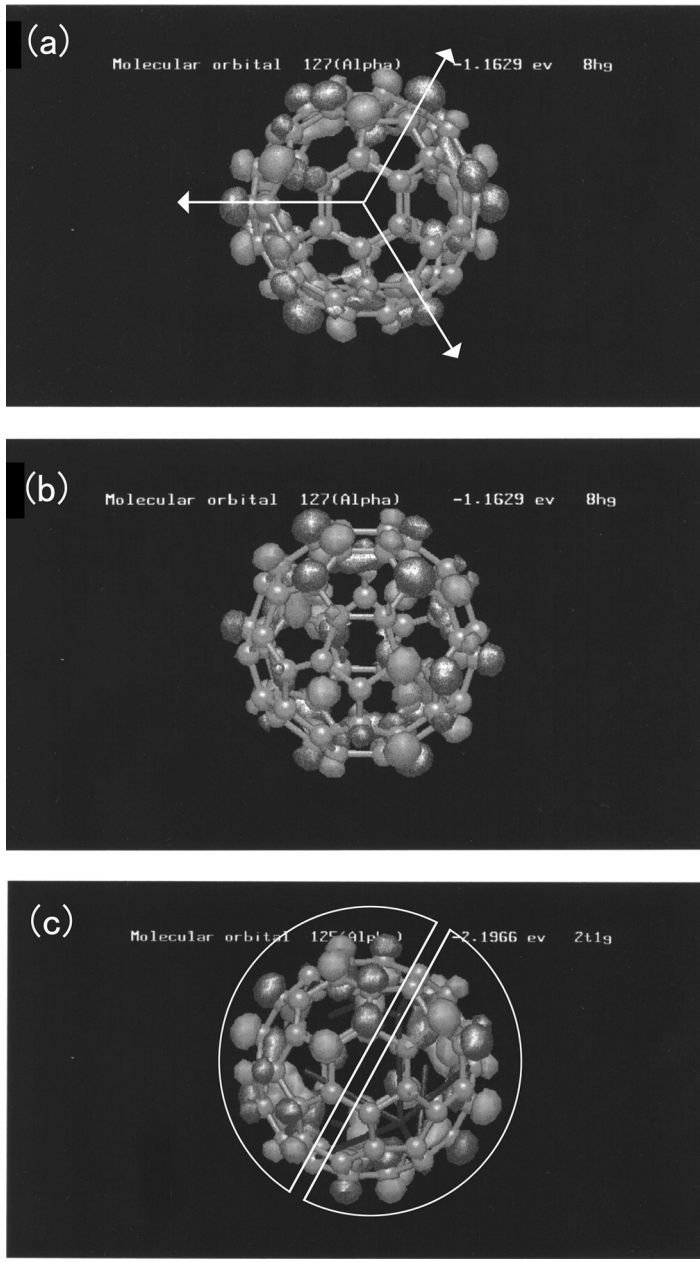

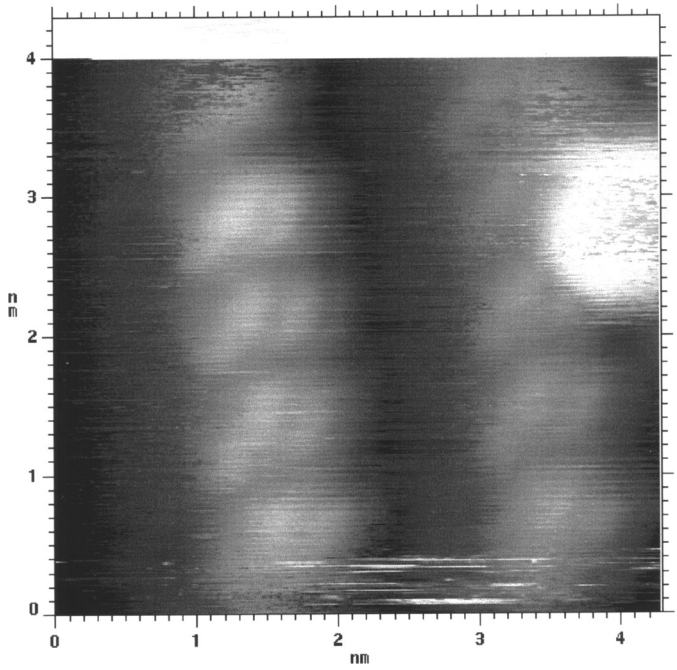

FIGURE 10 STM image of a part of rubidium-doped C_{60} thin film, which shows one-dimensionally aligned orientation-fixed C_{60} molecules.

These findings clearly revealed the orientation ordering of C_{60} molecules in the crystal at low temperatures, typically 25 K.

Another subject is to clarify the crucial effect of alkali metal doping to C_{60} crystals. In the rubidium-doped C_{60} films, the interaction between C_{60} molecules and rubidium ions may interrupt the rotation of C_{60} molecules and causes a merohedral ordering of the molecular orientation in the crystal even at room temperature. Furthermore, the STM images of some parts of the film exhibited one-dimensionally aligned structure of C_{60} molecules induced by the doping (Fig. 10).

The last subject of this report is an STM/STS study on the metallic nature of alkali metal C_{60} complex solids. Alkali metal-doped C_{60} solids have been known to be metallic conductors and superconductors at low temperatures when they are properly doped. The main role of alkali metal is believed to be the electron-donation to C_{60} molecules because of its relatively low ionization potential energy. In this work, we have aimed to clarify more detailed functions of the alkali metal to transform the electronic character of the solid from insulator to metal

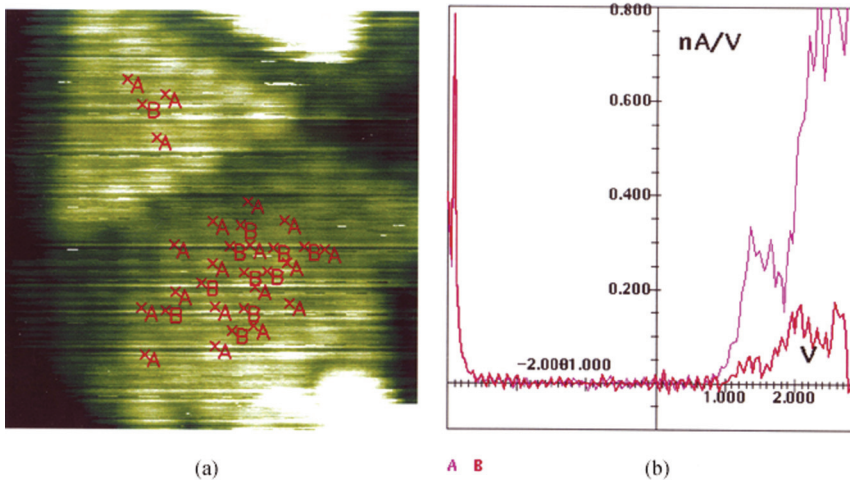

FIGURE 11 (a) STM image observed through the STS measurement for a genuine C_{60} thin film. x_A and x_B correspond to the site on the C_{60} molecule and the molecular interstitial site, respectively. (b) The site-selected tunneling spectra of the genuine C_{60} thin film obtained by STS measurement. The ordinate axis is the first derivatives of the tunneling current, and the abscissa is the bias voltages between the tunneling-tip and the sample. A (pink) and B (red) spectra correspond to the spectra for x_A and x_B sites, respectively.

by the doping reaction. We have directly observed the change of the electron density of states due to doping by applying an STS technique in the space- and energy-resolved way.

As the control experiment, the spatially resolved STS measurement was applied for a genuine C_{60} thin film, which is shown in Fig. 3. A typical result of the site-selected STS is shown in Fig. 11 where the x_A site and x_B site correspond to "on the molecule" site and "the molecular interstitial" site, respectively. Each spectrum in the right-hand figure (b) was obtained by averaging the all signals from x_A sites or x_B sites indicated in the left-hand figure (a). In the figure (b), the ordinate quantities are proportional to the electron density of the states and the abscissa ones are the energies of the molecular orbital. Based on these spectra, the so-called HOMO-LUMO gap was estimated to be about 3.5 eV, and the electron-density of the states on the molecule is reasonably higher than that of molecular interstitial sites.

The rubidium doping was carried out by the deposition of the proper amount rubidium vapor on the C_{60} film so as to prepare Rb_3C_{60} composite. The comparison of the intermolecular distances in the pristine

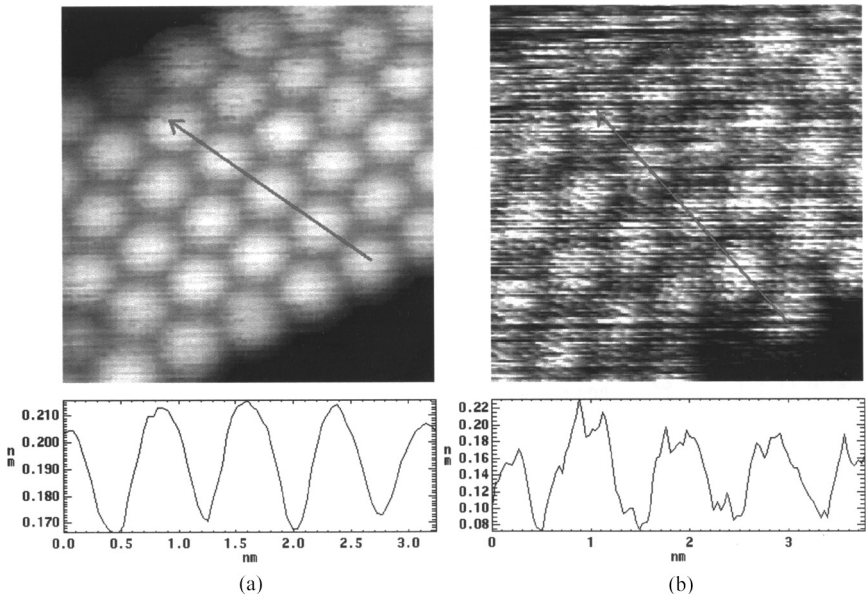

FIGURE 12 Comparison of the intermolecular distances in the pristine C_{60} thin film (a) and in the rubidium-doped C_{60} thin film (b). The side-sectional views of the surface height along the red lines in each picture are shown in the lower part of the figure.

C_{60} film and rubidium-doped one is shown in Fig. 12, which indicates clear expansion of the distance from ca. 0.8 nm in the genuine film to ca. 1.0 nm in the doped film. Further, the observed peak separations in the side-sectional-view of the doped film are possibly due to Rb ions incorporated in the film.

A typical result of the site-selected STS measurements for the rubidium-doped C_{60} films is shown in Fig. 13 in which A site means the site on the C_{60} molecule and B site means the molecular interstitial site. The STM image (a) in this figure was so poor in quality that a separate STM image at the same place was taken into account to identify the A site and B site. The remarkable change in the B-site spectrum in Fig. 13 compared with that in Fig. 11 is the enhancement in the electron density of states around the low-energy region (near Fermi level) due to doping, which results in the disappearance of the energy gap (HOMO-LUMO gap). On the other hand, the A-site spectrum in this figure is almost similar to that in Fig. 11. Further, some differences in the B-site spectra were also found depending on the local interstitial structures. These findings indicate that the change in the

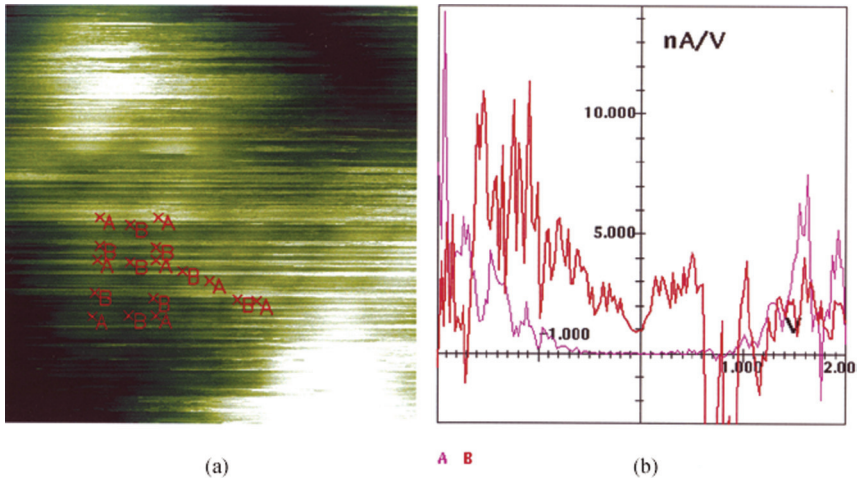

FIGURE 13 (a) STM image observed through the STS measurement for rubidium-doped C_{60} (Rb_xC_{60}) film: x_A and x_B correspond to the site on the C_{60} molecule and the molecular interstitial site, respectively. (b) The site-selected tunneling spectra of Rb_xC_{60} thin film obtained by STS measurement. A (pink) and B (red) spectra correspond to the spectra for x_A and x_B sites, respectively.

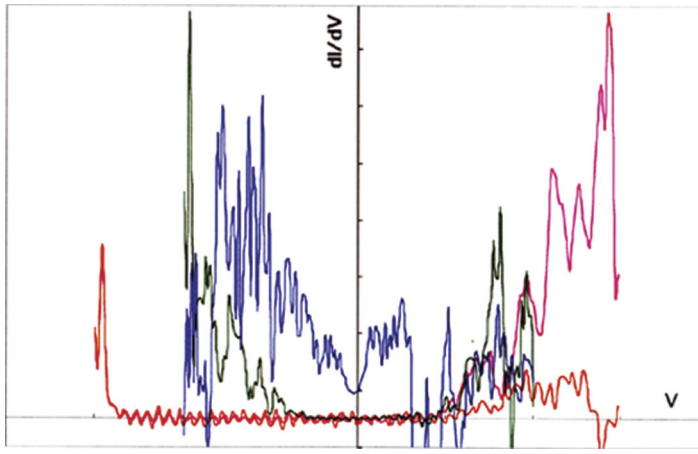

FIGURE 14 Summarized spectra of the site-selected local electron density of states: the pink curve: on the molecule site of the pristine C_{60} film; the orange curve: at the molecular interstitial site of the pristine C_{60} film; the green curve: on the molecule site of the Rb_xC_{60} film; the blue curve: at the molecular interstitial site of the Rb_xC_{60} film.

electron density of states is caused by the hybridization of the wave functions of C_{60} molecule and those of the interstitially doped rubidium ions, and this change in the electron density of states is the main origin for the appearance of the metallic nature in the rubidium-doped C_{60} crystals.

Finally, Fig. 14 shows the summarized result of the four spectra, which are A-site and B-site spectra of pristine C_{60} thin film and those of rubidium-doped C_{60} thin film. In this figure, the peak heights are normalized to coincide with the highest peaks in each A spectrum. Thus, these spatially resolved STS studies clearly indicate the possible hybridization of the wave functions of rubidium ions with those of C_{60} molecules, and it is an origin of the metallic nature of the doped-C_{60} crystals.

CONCLUSION

The orientation ordering of C_{60} molecules in the crystal at low temperatures has been revealed for the first time by the STM analysis for C_{60} crystalline thin films at ~ 25 K, and the observed result was visually illustrated and compared with that of molecular-orbital calculation for the C_{60} molecule. On the other hand, it was found by the site-selected STS measurements that the occurrence of the metallic nature in the rubidium-doped C_{60} crystal is reduced to the creation of new electron density of states at around the Fermi level of the doped crystal due to the hybridization of the wave functions of C_{60} molecules and rubidium ions at the molecular-interstitial regions.

REFERENCES

[1] Kratschmer, W., Lamb, L. D., Fostiropoulos, K., & Huffman, D. R. (1990). *Nature*, *347*, 354.
[2] Yannoni, C. S., Johnson, R. D., Meijer, G., Bethune, D. S., & Salem, J. R. (1991). *J. Phys. Chem.*, *95*, 9.
[3] Heiney, P. A., Fischer, J. E., McGhie, A. R., Romanow, W. J., Denenstein, A. M., McCauley, J. P. Jr., Smith, A. B. III., & Cox, D. E. (1991). *Phys. Rev. Lett.*, *66*, 2911.
[4] David, W. I. F., Ibberson, R. M., Dennis, T. J. S., Hare, J. P., & Prassides, K. (1992). *Europhys. Lett.*, *18*, 219.
[5] Hashizume, T., Wang, X.-D., Nishina, Y., Shinohara, H., Saito, Y., Kuk, Y., & Sakurai, T. (1992). *Jpn. J. Appl. Phys.*, *31*, L880.
[6] Hashizume, T., Motai, K., Wang, X. D., Shinohara, H., Saito, Y., Maruyama, Y., Ohno, K., Kawazoe, Y., Nishina, Y., Pickering, H. W., Kuk, Y., & Sakurai, T. (1993). *Phys. Rev. Lett.*, *71*, 2959.
[7] Kochansky, G. P., Hebard, A. F., Haddon R. C., & Fory, A. T. (1992). *Science*, *255*, 184.

[8] Haddon, R. C., Hebard, A. F., Rosseinsky, M. J., Murphy, D. W., Duclos, S. J., Lyons, K. B., Miller, B., Rosamilla, J. M., Fleming, R. M., Kortan, A. R., Glarum, S. H., Makhija, A. V., Muller, A. J., Eick, R. H., Zahurak, S. M., Tyco, R., Dabbagh, G., & Thiel, F. A. (1991). *Nature*, *350*, 320.
[9] Benning, P. J., Stepniak, F., Poirier, D. M., Martins, J. L., Weaver, J. H., Chibante, L. P. F., & Smalley, R. E. (1993). *Phys. Rev.*, *B47*, 13843.